

Determination of the source location of anthropogenic radionuclides collected in Finland and Sweden in June 2020 using a multi-technology analysis

Ian Hoffman^{a,*}, P. Mekarski^a, A. Botti^a, J. Yi^a, A. Malo^b, C. Cochrane^c, V. Khotylev^c, J. Kastlander^d, A. Axelsson^d, A. Ringbom^d, M. Moring^e, T. Karhunen^e, A. Mattila^e, M. Goodwin^f, A. Davies^g, K. Ungar^a

^a Radiation Protection Bureau, Health Canada (HC), 775 Brookfield Rd. Ottawa, ON, Canada

^b Environment and Climate Change Canada (ECCC), 2121, route Transcanadienne, Dorval, QC, Canada

^c Canadian Nuclear Safety Commission (CNSC), 280 Slater Street, Ottawa, ON, Canada

^d Totalförsvarets Forskningsinstitut (FOI), SE- 164 90 Stockholm, Sweden

^e Radiation and Nuclear Safety Authority, Finland (STUK), Jokiniemenkuja 1, 01370 Vantaa, Finland

^f Atomic Weapons Establishment (AWE), Reading, Berkshire, RG7 4RS, UK

^g Comprehensive Nuclear-Test-Ban Treaty Organization (CTBTO), Vienna International Centre, P.O. Box 1200, 1400 Vienna, Austria

ARTICLE INFO

Keywords:

Anthropogenic radionuclides
Atmospheric transport and dispersion models
CTBT
Coincidence spectroscopy

ABSTRACT

In June 2020, observations of anthropogenic radionuclides in Estonia, Finland, and Sweden that were not related to any acknowledged environmental release led to a comprehensive investigation on the source and cause of the unusual emissions. Several of the observed radionuclides were on the list of Comprehensive Nuclear-Test-Ban Treaty (CTBT) relevant radionuclides as an indicator of a potential nuclear test, and warranted detailed investigation. While analysis of aerosol samples coupled with Atmospheric Transport and Dispersion Modelling (ATDM) is a standard approach for environmental particulate releases, several new techniques were employed to better characterize the samples that allowed for useful inferences to be made. These inferences were crucial in forming the ultimate hypothesis for determining the facility type and location of the release.

1. Introduction

In June 2020, anthropogenic radionuclides including ^{106}Ru , ^{46}Sc , ^{103}Ru , and ^{137}Cs were initially observed at multiple locations in Estonia, Finland, and Sweden. The release went unacknowledged by any national nuclear authority, even after the International Atomic Energy Agency (IAEA) made requests from its member states for any information regarding the cause and possible source of these radionuclides. This incident occurred after a similar observation of ruthenium isotopes was observed in 2017 (Cooke et al., 2020; Masson et al., 2019; Hopp et al., 2020), which was convincingly postulated to be caused by an accident involving the failed production of a ^{144}Ce neutrino source at the Mayak nuclear facility for an experiment at the Gran Sasso national underground laboratory (Altenmüller et al., 2016; Istituto Nazionale di Fisica Nucleare, 2021; Vivier et al., 2016).

There is an international treaty in a preparatory phase, the CTBT,¹ that maintains a list of 83 fission and activation radionuclides

that are considered potential indicators of a nuclear test. The list is made of radionuclides that have suitable qualities (half-life, fission yield, gamma yield, history of detection) to be detected by a global network of verification equipment, the IMS. The IMS verification network relies upon two different technologies of environmental monitors. The first are seismo-acoustic (seismic, hydroacoustic, infrasound) and the second are radionuclide (aerosol and noble gas sampling). The nuclides detected were all on the list of relevant radionuclides, making this an event of interest for CTBT verification. If the treaty had been in force, the presence of these nuclides on aerosol filters may have resulted in a request for an On-Site Inspection (OSI), an expensive and time-consuming endeavour where an inspection team visits a designated area to search for evidence of a nuclear test. Applying a range of techniques, including some that are not part of the standard procedures of the Comprehensive Nuclear-Test-Ban Treaty Organization (CTBTO), which only include single detector gamma spectroscopy, allows for a fuller

* Corresponding author.

E-mail address: ian.hoffman@hc-sc.gc.ca (I. Hoffman).

¹ <https://www.ctbto.org/>.

exploration of the samples and data and could potentially avoid the OSI process.

This event had only a single detection at an IMS location in Stockholm, Sweden (CTBT code: SEP63) with the remaining detections occurring at national monitoring sites. The initial species of radionuclides identified were augmented with isotopes of Ce, Nb, Zr, Cs after further laboratory analyses as described in Section 2. These additional radionuclides are also all on the list of CTBT relevant radionuclides, and the complete set of radionuclides detected were much more likely to be associated with an atmospheric nuclear test than leakage from an underground test. The Ru, Ce, Cs and Nb species are fission products, while Zr can be produced through both fission and activation mechanisms. The only definitive activation product was Sc, which has also been observed in nuclear fallout (Krieger and Groche, 1960). The combination of nuclides detected and the lack of any other evidence such as a direct visual observation or associated infrasound signal of an atmospheric test meant that a nuclear test was not viewed as a source of the radionuclides, however the Canadian, Swedish, Finnish, and UK National Data Centres (NDC), who independently analyse environmental radionuclide data for potential CTBT violations, were interested to perform a thorough investigation of this incident and see if a probable source could be identified and better understand the characteristics of this release event.

One of the main challenges with unacknowledged release incidents is that there are often many possible sources, and it can be hard to know which of the sources are reasonable candidates. This study was conducted to see how the available information could be used to make inferences about the source to see how many possible sources could be eliminated and if an overall assessment of the source is possible. To arrive at our conclusion for the cause of this incident, a multi-disciplinary approach was required that made use of aerosol filter measurements of radionuclides, coincident spectroscopy, Atmospheric Transport and Dispersion Modelling (ATDM), nuclear reactor burn-up codes, knowledge of historical radionuclide background activity concentrations and industrial activities.

2. Method

With limited aerosol samples many of which were one week samples, it can be difficult to establish a candidate source location as the atmosphere changes greatly over the course of a week and the plume passage can be a small fraction of the sampling interval. Such scenarios are difficult to analyse from an activity concentration measurement (using a single detector) of the aerosol samples. In order to make useful inferences many other techniques, including multi-spectrometer measurement, auto-radiography, reactor fuel modelling, ATDM and an examination of the historical concentrations of observed radionuclides were applied in this study.

Due to the number of samples available during this event, the radionuclide laboratories collaborated by using applying different analytical techniques and sharing the results of their analyses with the others. The first analyses were laboratory (re)measurement of the radionuclide content of the field aerosol filters. The laboratory analysis of these environmental samples were the first to indicate that there was anthropogenic radionuclides present and they were unusual. After the initial analysis several other analyses were conducted by different laboratories in an attempt to understand the nature of the release. By using autoradiography (Finland), and a dual germanium detector system (Canada, UK), the homogeneity of the samples could be examined to see if the physical characteristics of the deposited material could be used to infer the properties of the source.

2.1. Radionuclide field and laboratory measurements

Several aerosol samplers from the region had collected one or more anthropogenic radionuclides. The location of the aerosol samplers used in this study is shown in Fig. 1. The IMS sample collected in Stockholm, Sweden and the Helsinki samples were initially analysed on-site (Samples 1 and 4 in Table 1) using a high-resolution germanium spectrometer while the remaining samples were sent to central laboratories responsible for environmental aerosol monitoring in their respective countries for analysis. Following the initial detection of anthropogenic radionuclides, the Helsinki sample was sent to the Finnish national lab for an extended acquisition period of 48 h (on-site measurements are 24 h) that resulted in the detection of additional anthropogenic radionuclides. Furthermore, since the IMS sample from SEP63 had at least one fission and the presence of activation products, it was split into two pieces and sent to two different laboratories for reanalysis (following the standard CTBTO procedures).

For all IMS aerosol samples, the NDC of Canada, Finland, Sweden, and the United Kingdom all receive and process the raw spectrometry data. The Canadian NDC performs its own analysis of the spectra in-house using the Unisampo-Shaman software that is coupled to a LINUX System for Spectral Information (LINSI)² database. The sample collection parameters and initial laboratory analyses of all samples are shown in Tables 1 and 2. The samples available for this study were collected for h24 periods, or in the case of various national samplers, for durations of up to a week.

2.2. Sample physical characterization using auto-radiography and multi-detector spectroscopy

Auto-radiography is an analytical technique sensitive to β and α particles which show up as dark spots on a phosphor imaging plate which are then digitally scanned. Auto-radiography has useful applications for nuclear forensic investigations (Parsons-Davis et al., 2018). In this study auto-radiography was used to examine the physical particles present on the aerosol filter collected at Helsinki.

Health Canada (HC) has a special dual-germanium detection system that includes a cosmic veto for background suppression called *Thin Man*. The *Thin Man* system is an operational version of the system described in Zhang et al.. The system has two Mirion BEGe 5030 detectors mounted horizontally inside a graded shield with a sample holder in the middle. The shield is 12.7 cm of lead with a tin and copper liner. Borated polyethylene with a thickness of 2.54 cm is used for neutron absorption. Plastic scintillators surround the sides and top of the detection system to provide an active cosmic veto. Two time-synchronized Mirion Lynx Multi Channel Analyser (MCA) were used for initial signal processing, with the data acquired and analysed in list mode by custom software to provide anti-coincidence, coincidence, summed spectra and individual detector spectra within a single counting period. This more detailed examination technique allowed for the variations in response of each detector to the radioactive material deposited on the filter to provide additional physical characterization of some of the samples.

Sample 2 was measured by AWE on their dual detector system, which is very similar to the *Thin Man* system described above, while sample 5 was measured at HC. The use of this system allows for greater sensitivity and specificity of the radionuclides present in a sample. The combination of dual detection (with nuclides that have an appropriate cascade decay scheme), allows for much greater abilities to detect trace materials as the background and interferences are greatly suppressed. Furthermore, the requirement of a cascade in the decay scheme means that the analyst can be very certain about the identification of radionuclides present in the sample (Britton and Davies, 2019).

² See <http://linssi.hut.fi/> for more details.

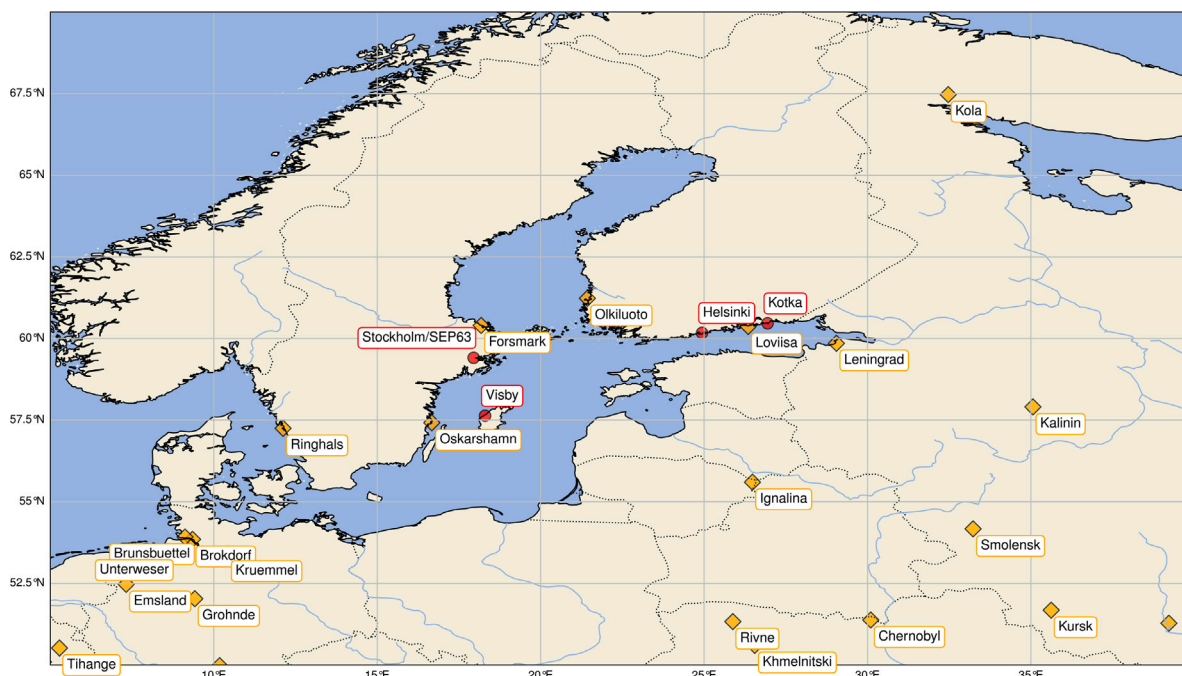


Fig. 1. The names and locations of the samplers (red circles) that detected anomalous anthropogenic radionuclides in June 2020. The names and locations of regional nuclear power plants (yellow diamonds) are shown to indicate possible NPP sources of the detected fission products. (For interpretation of the references to colour in this figure legend, the reader is referred to the web version of this article.)

2.3. Reactor core modelling

The anthropogenic radionuclide content was also examined from a fission production simulation performed by Canadian Nuclear Safety Commission (CNSC). This type of analysis can indicate the type of reactor by considering ratios of interdependent fission product chains and can calculate the time since fuel discharge from the reactor core. The computer code, SCALE v6.0,³ is a simulation tool used in criticality safety, reactor physics, radiation shielding, radioactive source term characterization, sensitivity and uncertainty analysis. For this study, SCALE was used by CNSC to model the evolution of reactor fission products and to estimate the time since fuel discharge from the reactor.

2.4. Atmospheric Transport and Dispersion Modelling (ATDM)

The radionuclides travelled as aerosols from a source location to several detection points as indicated in Fig. 1, and simulations of the atmospheric transport conducted by Environment and Climate Change Canada (ECCC) were examined using retro-plumes to narrow down the source region and identify candidate facilities.

2.5. Historical observational records

Finally, since the history of radionuclide observations at Visby were provided by Sweden and was considered in the interpretation of the results. Radionuclides such as ^{137}Cs , have very long half-lives so that multiple sources (e.g. legacy nuclear test material) can be responsible such as during forest fire season when radionuclides entrapped in vegetation become mobilized in the air. Examining relative isotopic concentrations of radionuclides can lead to incorrect conclusions when multiple sources can contribute to the contents measured in the aerosol sample.

3. Results and discussion

3.1. Initial aerosol analysis

The first results from the field are shown in Table 1. The radionuclides measured were a mixture of fission and activation products that have been seldom measured in the environment.

Due to the nature of these radionuclides the field samples were measured at central laboratories for longer durations and the extra time between sample collection and measurement allowed the radon progeny to decay further and improved the sensitivity of the counting process.

Based on the initial analysis of both field measured and laboratory remeasured samples, the richest set of nuclides were observed in Helsinki, Finland (Sample 1). This suggests that the source was closer in transport to this location. Overall, the timing and general commonality of nuclides in the set of samples collected suggested a common source. However, analysis of the $^{134}\text{Cs}/^{137}\text{Cs}$ ratios was highly variable between the samples as shown in Table 3. The wide range of ratios was difficult to explain through statistics or re-suspension of historical ^{137}Cs and will be examined in greater detail in Section 3.2, where the filters were examined using an auto-radiographer, and in Section 3.6, where the historical background levels of Visby, Sweden are examined.

3.1.1. Detailed analysis of visby sample (5)

One of the samples from Visby was examined to characterize the ruthenium production characteristics, since these isotopes are rarely seen in the environment. The last notable aerosol observations of ruthenium occurred in 2017, and a plausible Russian source was identified (Cooke et al., 2020; Ramebäck et al., 2018). Using Sample 5 from Visby, we examine the anthropogenic radionuclide contents of the filter in terms of its cumulative fission product yield (thermal) and the production of ^{103}Ru and ^{106}Ru during nuclear fission. The relevant parameters are shown in Table 4. Although it is possible for some reactors to burn Mixed Oxide Fuel (MOX), it normally requires a re-licensing process due to changes in the core reactivity, and is not

³ <https://www.ornl.gov/content/scale-v6>.

Table 1
Sample collection parameters from IMS and national aerosol samplers.

Sample number	Location	Collection start (UTC)	Collection stop (UTC)	Nominal duration (d)	Sample volume (m ³)
1	Helsinki	2020-06-16 08:00	2020-06-17 07:45	1	12 579
2	Visby	2020-06-08 08:00	2020-06-15 07:45	7	97 950
3	Stockholm	2020-06-21 23:57	2020-06-23 03:57	2	32 410
4	SEP63	2020-06-22 08:58	2020-06-23 08:56	1	12 947
5	Visby	2020-06-15 07:45	2020-06-22 09:45	7	98 682
6	Kotka	2020-06-15 00:00	2020-06-22 00:00	7	92 964
7	Stockholm	2020-06-23 03:57	2020-06-24 07:57	1	31 905

Table 2
Initial laboratory measurements reported in Sweden and Finland. One-half of the IMS (SEP63) sample was analysed at the CTBT certified laboratory in Ottawa, Canada (quoted here). The remaining samples were analysed at national laboratories in their respective countries.

Sample number	Activity concentration (μBq m ⁻³)							
	¹³⁷ Cs	¹³⁴ Cs	⁶⁰ Co	¹⁰³ Ru	¹⁰⁶ Ru	⁹⁵ Nb	⁹⁵ Zr	¹⁴¹ Ce
1	11.00(66)	15.0(6)	6.10(31)	1.90(32)	<9.9	3.70(30)	2.10(17)	1.70(24)
2	1.340(75)	0.77(4)	0.22(5)	0.100(42)	<1.85	<0.25	<0.4	<0.56
3	<0.33	<0.64	0.39(14)	<0.54	<1.2	<0.67	<1.0	<0.74
4	9.01(47)	11.08(66)	<4.290	3.98(27)	<37.13	<3.403	<5.457	<5.526
5	0.690(67)	0.620(42)	0.360(68)	0.730(69)	1.37(69)	0.830(78)	0.570(58)	<0.43
6	2.40(12)	1.700(51)	0.700(35)	0.300(24)	<6	0.400(28)	0.300(24)	0.200(34)
7	0.710(67)	0.310(48)	<0.53	<0.43	<3.8	<0.54	<0.84	<0.64

Table 3
¹³⁴Cs/¹³⁷Cs ratio. The relative amounts of these two radioisotopes can give an estimate of the genesis time of the isotopes and an indication of whether historical ¹³⁷Cs was present. For reference, samples from the Fukushima reactor accident had a ratio of approximately 1.2.

Sample number	¹³⁴ Cs/ ¹³⁷ Cs
1	1.36
2	0.57
3	
4	1.23
5	0.90
6	0.71
7	0.44

Table 4
Half-life and cumulative thermal fission yield (IAEA, 2022).

Species	Half-life (d)	²³⁵ U (%)	²³⁹ Pu (%)
¹⁰³ Ru	39.247(13)	3.10(8)	6.95(8)
¹⁰⁶ Ru	371.8(18)	0.410(11)	4.19(9)

viewed as likely fissile material, so this work will focus on ²³⁵U fission. For a given neutron flux, the production of ¹⁰³Ru will be greater than that of ¹⁰⁶Ru, and ¹⁰⁶Ru will also reach equilibrium slower than ¹⁰³Ru.

In a reactor, the ¹⁰³Ru/¹⁰⁶Ru ratio starts large and decreases slowly throughout the irradiation period and subsequent decay after removal from the core. The production process in terms of the number of atoms produced, A_n , for simple neutron irradiation is given in Eq. (1), with Φ being the neutron flux, σ_f , the thermal fission cross-section, f_n , the thermal fission product yield, N_d , the number density of fissionable atoms, λ_n , the decay constant, and t , the duration of irradiation.

$$A_n = \Phi \sigma_f f_n N_d (1 - e^{-\lambda_n t}) \quad (1)$$

It is helpful to examine both limiting cases ($t \rightarrow 0$ and $t \rightarrow \infty$) in terms of the ¹⁰³Ru/¹⁰⁶Ru activity ratio. Assuming a ²³⁵U source, and for short irradiation, Eq. (1) becomes the product of the relative fission product yields and decay constants, or 71.6(27). For the latter case of a long irradiation period, Eq. (1) is simply the ratio of the fission yields of the two isotopes, or 7.56(28). Once the target is removed from the reactor, ¹⁰³Ru decays much faster than ¹⁰⁶Ru ($\tau_{1/2} = 39.247$ d and $\tau_{1/2} = 371.8$ d respectively), and therefore the activity ratio decays exponentially, with a resulting half-life of 43.879(29) d.

The starting ratio (at fuel discharge) will have been between the limiting values above. Furthermore, the shorter the irradiation period, the

longer it will take to reach the activity ratios reported in Table 5. From these inferred constraints, and the evolution of the activity ratio, the post-irradiation decay period would be significantly less than a year. Although the irradiation time is the determining factor in the evolution of the ratio, a calculation was done by Totalförsvarets Forskningsinstitut (FOI) using SCALE to examine if the behaviour would change depending on the type of fuel (Highly Enriched Uranium (HEU) or Low Enriched Uranium (LEU)). A VVER with low enrichment was simulated with 35 MW t⁻¹ was compared to metallic HEU at 650 MW t⁻¹. With fresh fuel, and an irradiation time of 10 d, both fuels took around 250 d to reach a value near unity. A more detailed analysis of the irradiation, activity ratio and discharge time is presented in Section 3.5 when a full core model of both an Reaktor Bolshoy Moshchnosti Kanalnyy (RBMK) and VVER reactor was used along with the relative amounts of anthropogenic radionuclides observed.

3.2. Auto-radiography

The Helsinki aerosol sample (1) was examined using an auto-radiographer by Radiation and Nuclear Safety Authority, Finland (STUK). The filter was from a Cinderella type sampler with a glass fibre filter comprised of 15 stacked sheets.⁴ The results of the auto-radiography exposure is shown in Fig. 2.

Auto-radiography allowed for a qualitative examination of the filter and for inferences to be made regarding the radioactive particles that were captured on the sampling matrix. The images allow one to consider the particle size and overall radionuclide distribution on the filter. The auto-radiography results were compared to a historical analysis of Canadian samples previously collected in Yellowknife, Canada, that were very similar from a radioactivity content except for the varying levels of ²¹⁰Pb (radon progeny) that oscillate seasonally depending on the presence and amount of snow pack. The analysis of a previous anthropogenic release event (Cooke et al., 2020) where highly dispersed RuO₄ became entrapped on a German Weather Service sample is shown in Fig. 3.

For auto-radiographs that are only impacted by ²¹⁰Pb from Yellowknife, there is a highly linear relationship between the activity concentration and the overall darkening of the exposure film. The filter with anthropogenic radionuclides is shown at the correct position according to its ²¹⁰Pb content but it is much darker due to the anthropogenic radionuclides that are also present. In contrast to Fig. 3, the

⁴ See <https://senya.fi/cinderellag2.php> for details.

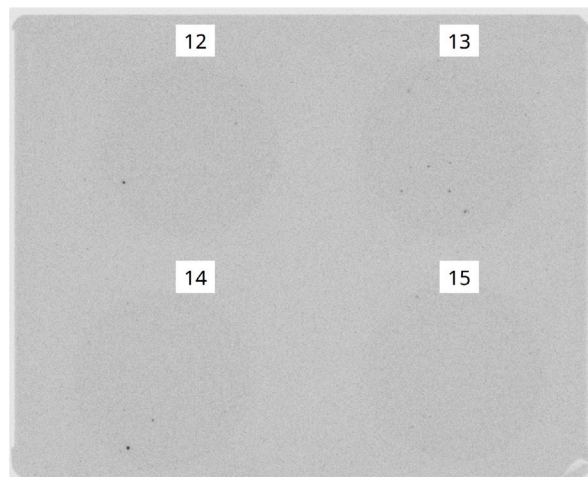


Fig. 2. An example of the sheets from the Cinderella sampler located in Helsinki (Sample 1). The filter sheets were analysed individually (the label is the sheet number) through auto-radiography. The anthropogenic radioactivity was contained in the small dark spots. The remaining other sheets (1 through 12) were similar.

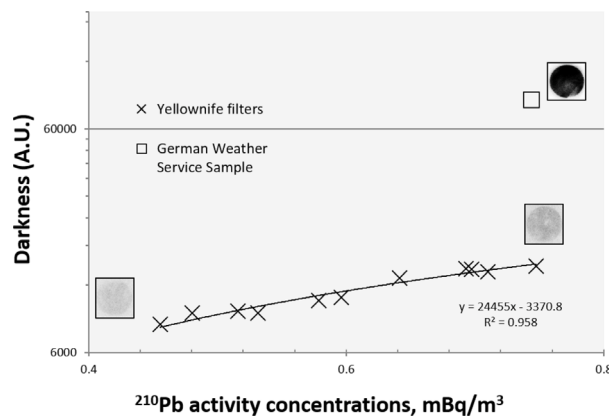


Fig. 3. Auto-radiography results for several aerosol samples containing various amounts of ^{210}Pb from filters collected in Yellowknife, Canada. The dark sample was from the German Weather Service during a different anthropogenic release event in 2017.

exposure of each layer of the Helsinki filter was very clean except for a few small particles per sheet, in total around 20 particles that contained the majority of sample radioactivity. This would seem to imply the release of discrete metallic fuel material rather than a highly dispersed RuO_4 release as has been previously observed as a result of reprocessing activities (Cooke et al., 2020).

3.3. Thin man multi-detector analysis

For CTBT samples, the current procedures involve field or laboratory measurement with a single germanium detector. This limitation means it can be much more difficult to perform verification especially when there are other non-destructive measurements available that improve verification capability tremendously through the physical characterization of the material on the filter and through the use of multi-detectors analysis which improves specificity and sensitivity of detection systems (Britton and Davies, 2019).

The Swedish Defence Research Agency, FOI, and the Finnish Radiation and Nuclear Safety Authority, STUK, supplied the Canadian laboratory with their national samples to conduct an in-house analysis of the filters. HC performed laboratory measurements using two different techniques on the separate filters from Helsinki and Visby. The first involved a detailed measurement of each sheet of the Helsinki sample using several single high-resolution detector systems at the radionuclide laboratory at HC and the second approach used a special dual germanium detection system. Both of these techniques were employed

to understand more of physical nature of the deposition process to help with inferences about the event source and possible cause.

The Helsinki sample (1) was measured using a non-routine technique to examine the homogeneity of the entrapped radioactive debris. This Cinderella sample was analysed with each individual sheet measured separately rather than the normal practice of measurement the superposition of all sheets. The analysis of main anthropogenic radionuclides is shown in Fig. 4, while the homogeneity was further assessed in Fig. 5. The variation in anthropogenic radionuclides was clearly evident when compared with the natural radionuclides (^7Be , ^{210}Pb , ^{40}K) which had very consistent activity concentrations among the filter sheets. In contrast, the anthropogenic material was highly variable in terms of concentration. For example, the $^{134}\text{Cs}/^{137}\text{Cs}$ ratio for the whole sample was 1.22 while it varied on an individual sheet from 0.76 to 1.94, providing further evidence of the inhomogeneous nature of the debris.

Following the initial analysis and auto-radiography (see Section 3.2), samples from Finland and Sweden were analysed at AWE on their dual detector system and at HC using the *Thin Man* system. The Visby sample that HC received was analysed in whole and then was quartered to investigate homogeneity of the radioactive debris present. The decision to examine a quarter piece was made based upon the auto-radiography results that showed significant differences in particle distribution on the filter.

Measurement on the dual detector system allowed for definitive identification of the radionuclides having cascading decays and also allowed for the identification of additional radionuclides due to the

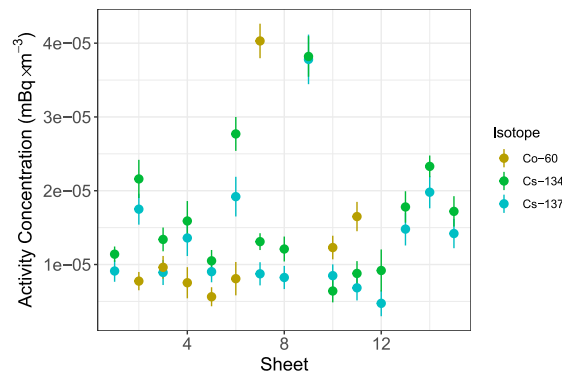


Fig. 4. The main anthropogenic radionuclides were analysed by filter sheet. From this analysis, the radioactive debris appeared to be in discrete particles as the activity concentration varied widely among the 15 sheets of filter.

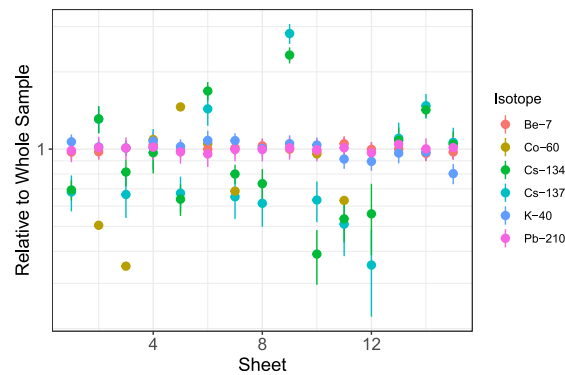


Fig. 5. The nuclides in each sheet were assessed relative to the overall sample activity. Two common natural radionuclides were included so that the sample collection behaviour could be examined relative to these well-dispersed natural radionuclides.

Table 5
Analysis of the baltic samples with *Thin Man* and AWE dual gamma systems. The Visby sample, was measured in whole (5W) and a quarter piece (5Q).

Sample number	¹³⁴ Cs/ ¹³⁷ Cs	¹⁰³ Ru/ ¹⁰⁶ Ru	⁹⁵ Nb/ ⁹⁵ Zr	¹⁴¹ Ce/ ¹⁴⁴ Ce
1	1.222(20)	0.877(89)	1.614(123)	0.573(41)
2(AWE)	0.637(36)			
5W	0.810(23)	0.929(96)	1.358(42)	0.825(29)
5Q	0.965(29)	0.865(69)	1.589(56)	0.653(24)

enhanced sensitivity of the system. Furthermore, analysis with the dual detector system allowed for a more precise determination of nuclide ratios that are given in Table 5. The confidence interval for the activity ratio were calculated using Fieller’s theorem (Fieller, 1954) which gives an approximate confidence interval if an assumption of normality can be made. However, since some of the activities were near the critical limit, L_c , the assumption of normality may not hold in all cases. However, in the interpretation of the ratios, this is unlikely to change the overall conclusion.

The use of this dual detector system added an additional four radioisotopes, ¹⁴¹Ce, ⁴⁶Sc, ¹⁴⁴Ce, and ^{110m}Ag, to the number of isotopes that were previously detected. These additional four radioisotopes were below the detection limit of a single detector, and their presence became very important when trying to understand the nature of the event and release. This ability to add additional radionuclides through an advanced laboratory measurement provided valuable information in understanding the source of the event as will be discussed in Section 3.5.

The other advantage of this system is that it very directly provides an assessment of sample homogeneity. Each detector will respond slightly differently to the anthropogenic materials on the opposing faces of the filter, due to self-shielding from the sample and due to the

nature of the materials on the filter. For this event, the anthropogenic material was comprised of larger discrete particles that were not homogeneously collected on the filter media. In contrast, the detectors will have an almost identical response to the natural radioisotopes (i.e. ⁷Be, ²¹⁰Pb, ⁴⁰K, ²²Na) present, as the natural particles are uniformly mixed throughout the air volume sampled and therefore more homogeneous in their collection on the filter media. This behaviour is apparent in the analysis shown in Fig. 6. One important detail to note from this analysis is that fission products (e.g. cerium and ruthenium isotopes) had different ratios (enhanced on filter top) compared to fission/activation and activation products (e.g. ⁹⁵Nb, ⁶⁰Co). The relative differences in fission product biases among groups of isotopes also provide evidence of material being in different phases (e.g. ⁹⁵Nb and ⁹⁵Zr travelled together). Although not shown here, the dual detector system demonstrated that real-time summation of the detector signals was effective at removing the relative bias that occurs when measuring a single face of a sample.

The combination of auto-radiography and the dual detection system provided valuable insight that would allow for inferences to be made regarding the nature of the radioactive particles and their origin.

3.4. Atmospheric Transport and Dispersion Modelling (ATDM)

ECCC is the Canadian government department that is responsible for the provision of meteorological models to support the NDC. ECCC uses a model developed in-house called Modèle Lagrangian de Dispersion de Particules (MLDP)(D’Amours et al., 2015) for operational response activities, including CTBT related incidents. By performing adjoint modelling (i.e. time-reversed transport and dispersion where the air parcels are modelled from collection point backwards in space and time) from the collection sites, it is possible to constrain the source to a region, which would hopefully contain a single or several nuclear facilities. Typically, the more samples available in a reconstruction,

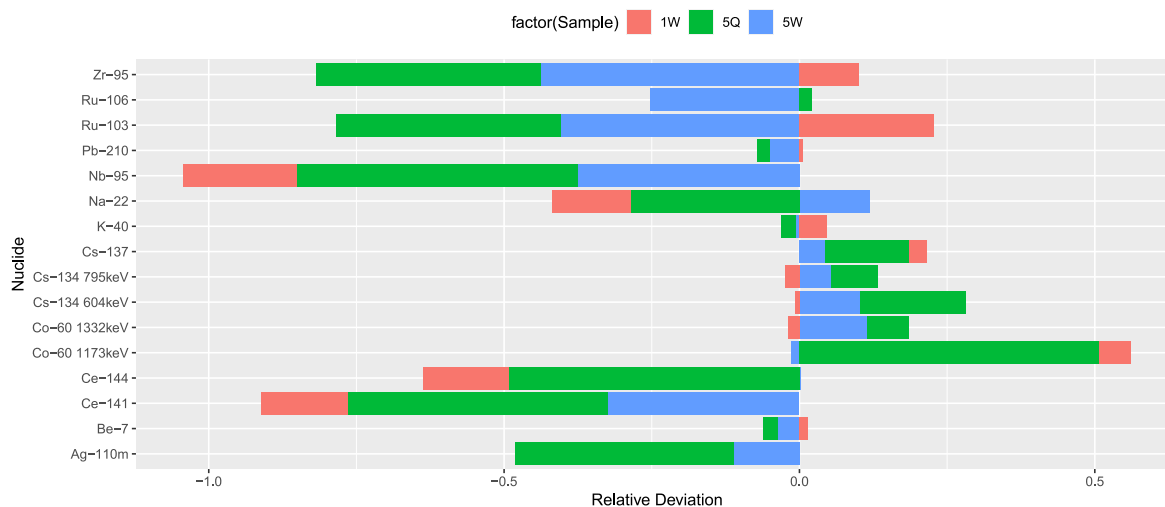


Fig. 6. The Helsinki and the whole (W) and quarter (Q) Visby sample (1; 5Q; 5W) were examined using a dual germanium system in list mode. The relative deviation from equal response on both detectors of the *Thin Man* system is shown. Natural radionuclides registered homogeneous responses (Deviation ≈ 0), while the anthropogenic radionuclides show a preferential bias indicating the radioactive debris was composed of a small number of discrete particles (with species in different phase groups) that showed up preferentially on either side of the sample. The lengths of the coloured bars give the relative inhomogeneity between the top and bottom of the sample. (For interpretation of the references to colour in this figure legend, the reader is referred to the web version of this article.)

the more constrained the potential source region will be. For regions with several candidate facilities, other information can be used to identify the source or at least narrow the number of possibilities that need further consideration, following the analyses used in [Cooke et al.](#), [Masson et al.](#)

ECCC performed adjoint modelling for all the daily detections reported in [Table 2](#) to assess the potential source region. Due to the magnitude of the detected activities and the material nature, the source had to be at meso-scale (10 km to 1000 km). A larger source would have resulted in many more detections throughout the region while a smaller source would have been very local and only detected near the point of origin. The small number of radioactive particles collected on the filters would also suggest a meso-scale release. The number and specific isotopes identified suggested a nuclear fission source rather than a laboratory, radio-therapy or radio-diagnostic source. The research facilities and nuclear reactors in the region ([Fig. 1](#)) were examined using ATDM to derive an upper bound sensitivity factor to limit the domain size during the selection of possible sources. The characteristics of the sparse filter debris meant that ATDM should not be used to infer the actual release size. ATDM models make an assumption that the aerosol particles are homogeneously dispersed throughout each air parcel modelled, and in this instance the particles were very inhomogeneous as was shown in [Fig. 6](#). Further development in the atmospheric modelling domain is required for releases having a small number of particles to accurately assess the source size.

To produce the ATDM assessment, a series of high resolution models were generated from all regional nuclear facility candidates. The initial meteorological analysis identified two nuclear facility locations as possible sources. This was determined through a spatial-temporal overlap from the detection sites and the nuclear facilities. The Leningrad and Kalinin nuclear plants were the likely locations of the release. The Ignalina plant was not considered a potential source as it had already been decommissioned. The Leningrad site has both RBMK and VVER reactor types while the Kalinin site only has the latter type.

High resolution models (5 km horizontal resolution) were generated for all daily sample measurements in [Table 2](#). A unit release of a depositing (wet and dry) particulate was released from both sites. The results of this analysis is shown in [Fig. 7](#). The figure shows the Leningrad site had more inter-sample consistency in terms of sensitivity to a fugitive release from a single location, while also showing greater sensitivity overall (a source 100 times smaller would be required to create the set of observations). While not conclusively a determination

of the source location, it is more probable considering both the consistency and smaller overall size necessary. Furthermore, the analysis also shows that there were likely two emission periods of radioactivity. Each period of sensitivity was roughly 1 d, but it is difficult to say conclusively how long material was released into the atmosphere.

The ATDM modelling is very powerful tool for illuminating the propagation considerations of fugitive releases, but it is not the only information available. Further evidence to help distinguish between the candidate source locations is available through modelling the fuel burn-up of the reactors. A model of the burn-up combined with the *Thin Man* dual detector analysis will hopefully support the ATDM source hypothesis.

3.5. Reactor core modelling

The CNSC is the Canadian government agency that is responsible for the regulation of nuclear energy and materials in Canada. As such, it has expertise in assessing the performance of nuclear reactors. Since the observed radionuclides were a mix of fission and activation products, a release from a NPP should be considered a potential source. The CNSC was engaged to model the fuel burn-up of the RBMK and VVER reactors to see if the ratios in observed radionuclides were characteristic of either reactor type. If the ratios were diagnostic of a particular type of reactor, that would further narrow down the list of possible sources, beyond the restrictions of a regional source due to the limitations imposed by the observations and corresponding ATDM. The CNSC made use of the HELIOS-2([Studsвик, 2008](#)) generalized-geometry lattice physics code to simulate the fuel burn-up and discharge of both reactor types. The presence of isotopic and isobaric pairs would hopefully allow for a characterization of the source material that could determine if either, both or neither reactor type was a suitable candidate for the observations. The four different isotopic pairs were considered in various combinations as given in [Table 6](#).

Fuel burn-up is impacted by local variation in neutron flux, with fuel elements near the centre of a fuel bundle exposed to a different neutron flux and energy spectrum compared to elements at the periphery. These differences in neutron environment results in changes to the fission product inventory, which could impact the overall assessment of isotope ratios. In [Figs. 8](#) and [9](#), the range of potential ratios due to fuel element location is represented through thickening of the burn-up evolution lines. It is also possible that the fuel was removed from the core prior to full utilization, but the behaviour shown in [Figs. 8](#) and [9](#)

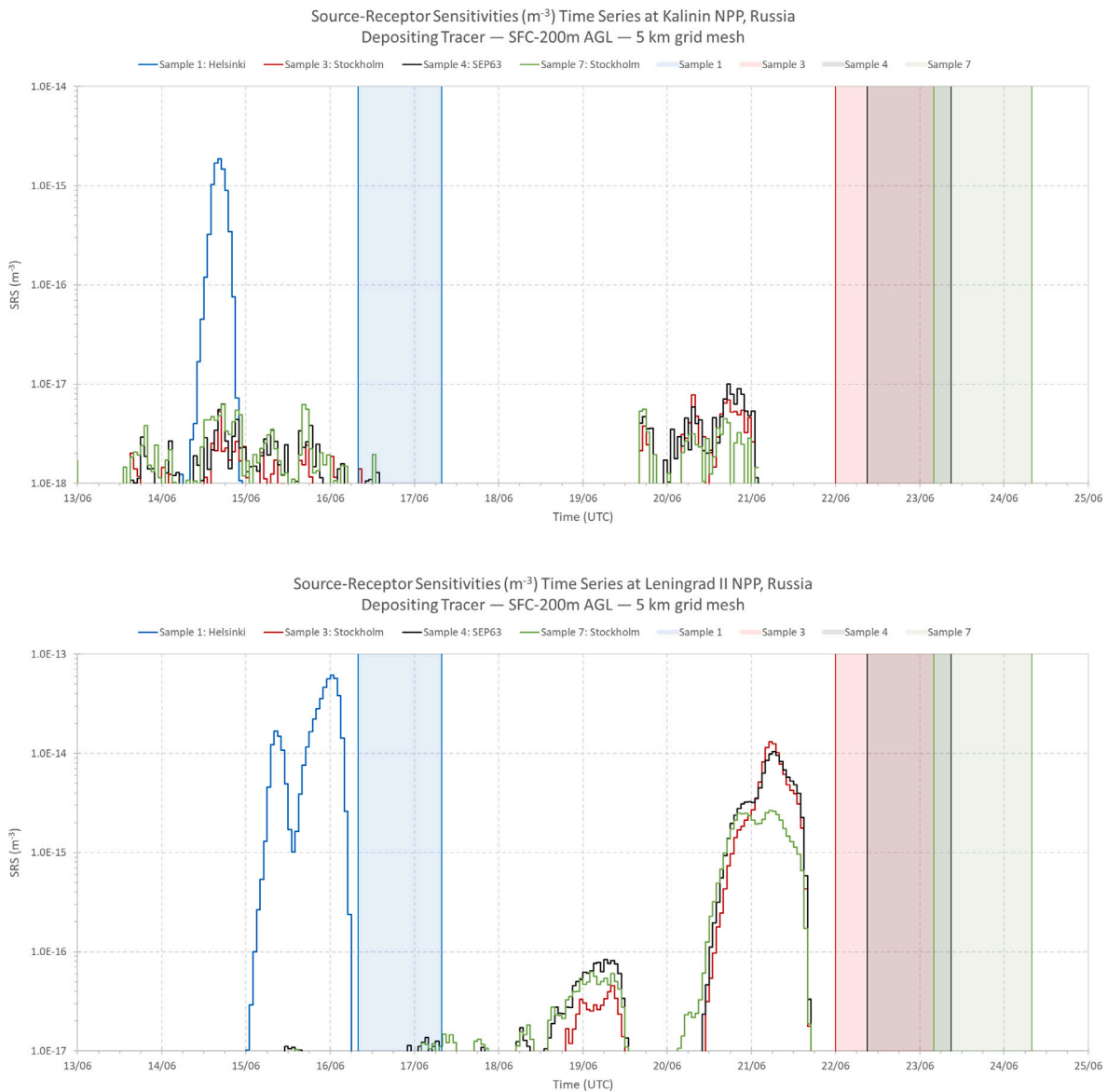


Fig. 7. The sensitivity of Kalinin (top) and Leningrad (bottom) to a release of well-dispersed particulate emission. Deposition both wet (based upon a parametrization of relative humidity) and dry was considered in the model. The coloured regions indicate the duration of sample collection periods from Table 2, with the earlier period showing sensitivity to Helsinki, while the later period shows the co-located samplers in Stockholm. The sensitivity plot shows a much greater sensitivity to Leningrad, indicating it is a more likely source as Kalinin would require a much larger release (accompanied by more detecting locations). (For interpretation of the references to colour in this figure legend, the reader is referred to the web version of this article.)

Table 6

The isotopic and isobaric pairs examined in reactor burn-up code, HELIOS-2, are listed.

Pair 1	Pair 2
⁹⁵ Nb/ ⁹⁵ Zr	¹⁰³ Ru/ ¹⁰⁶ Ru
¹³⁴ Cs/ ¹³⁷ Cs	¹⁰³ Ru/ ¹⁰⁶ Ru
⁹⁵ Nb/ ⁹⁵ Zr	¹³⁴ Cs/ ¹³⁷ Cs
⁹⁵ Nb/ ⁹⁵ Zr	¹⁴¹ Ce/ ¹⁴⁴ Ce
¹⁰³ Ru/ ¹⁰⁶ Ru	¹⁴¹ Ce/ ¹⁴⁴ Ce
¹³⁴ Cs/ ¹³⁷ Cs	¹⁴¹ Ce/ ¹⁴⁴ Ce

indicate that the fuel was removed at a time near normal fuel discharge and not earlier.

The pairs of cerium and ruthenium should be the clearest pairs of isotopes to interpret as both pairs have only a fission genesis mechanism, unlike ¹³⁷Cs, which may have historical remnants from previous

nuclear tests or ⁹⁵Nb, where both fission and activation through neutron capture is possible. This pair shown in Fig. 8, hints at a VVER origin particularly for the Helsinki sample, but the Visby sample was not fully conclusive due to the large uncertainties and lack of difference between the VVER and RBMK designs for these pairs.

The remaining pairs in Table 6 were now considered as shown in Fig. 9. The Helsinki sample shows ratios most consistent with the VVER reactor, while the Visby samples were more mixed. It is important to note that the ratios that rely upon ¹³⁷Cs are the most diagnostic, and that the presence of environmental ¹³⁷Cs can only move the ratios towards the RBMK reactor type (i.e. to lower values). It would also have been possible for the fuel to be removed from the core prior to its expected residence time (e.g. a fuel leak detected). This would have resulted in the fuel discharge regime of the ratio plot (ratio behaviour near the observations) occurring earlier in the plots. The observations and ratio evolution in both Figs. 8 and 9 show no clear evidence that the fuel was removed earlier than anticipated. In conclusion, the Helsinki sample provided clear support for a VVER origin, particularly with three

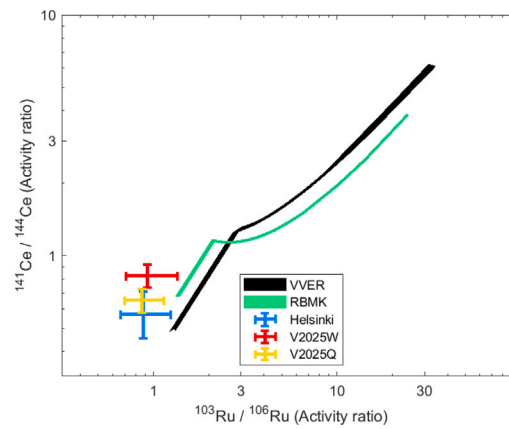


Fig. 8. The fuel burn-up from core insertion through to discharge is shown for the cerium and ruthenium isotopes. The Helsinki (whole and quarter sample) and Visby observed ratios are shown along with their associated uncertainty. The thickness of the fuel evolution shows the range of values possible due to the position of the fuel pin within the core.

of the four panels showing more definitive preference for a VVER origin, while the Visby samples are not fully conclusive or could indicate a mixed RBMK VVER source.

One last analysis was performed and that was a probability estimate of the release time of the debris since fuel discharge for both the RBMK and VVER reactor types. For each modelled point, a z -score was calculated comparing the measured value to the model value. As the values being compared are ratios, and uncertainties in ratios are distributed log-normally, the z -scores were calculated using the logarithm of the ratios. The uncertainty associated with the z -score, σ , is one quarter of the difference between the logarithm of the upper and lower 95 % confidence estimate of the measured values. The orientation of the deviation is not meaningful, so only the absolute value of the z -score is taken as shown in Eq. (2).

$$z = \left| \frac{\log(x_i) - \log(x_j)}{\sigma_j} \right| \quad (2)$$

The probability of measuring a deviation this far from the model is twice the complement to the normal cumulative distribution at that z -score. A z -score and associated probability is calculated for each measured ratio, and a joint probability is calculated by taking the product of the individual probabilities (a sum of the log probabilities). This approach assumes that each of the probabilities is independent (i.e. that the probability of measuring a given ratio of a given nuclide pair does not depend on the measurement of the other nuclides). This methodology is a synthesis of the methods presented in several peer-reviewed papers (Osborn et al., 2018; Charlton et al., 2000; Eslinger et al., 2019).

The probability of the release time is given in Fig. 10. Since the isotopic analysis is more consistent with a VVER, the most probable time since fuel discharge was approximately 51 d. At this early time, the fuel rod would normally have been in wet storage and would typically remain in the spent fuel pool for approximately five years.

3.6. Historical radionuclide activities and industrial activities

Observations of ^{137}Cs are challenging when performing an environmental interpretation due to the historical legacy of atmospheric nuclear testing. This becomes particularly true when considering the reactor modelling shown in Fig. 9 which relies upon interpreting ratios involving ^{137}Cs .

Aerosol sampling in Visby, Stockholm and Helsinki has been conducted for many years providing an assessment of typical environmental loads caused by re-suspension during forest fires.

Historically, ^{137}Cs is reported in Visby quite often, present at a few $\mu\text{Bq m}^{-3}$, which unfortunately is also consistent with the measured

amounts during this event. However, of the other radionuclides reported in Table 2, ^{46}Sc , ^{54}Mn , ^{95}Nb , ^{95}Zr , ^{110m}Ag , ^{134}Cs , ^{141}Ce , ^{144}Ce have not been observed in the Swedish monitoring network (6 sites) between 2012 and 2020 except during the period of this event. In 2017, ^{106}Ru was observed in aerosol, precipitation and soil samples in Sweden (Ramebäck et al., 2018). Lastly, ^{60}Co was observed on two occasions with weekly samples in 2013 and 2018, but no source was identified.

Although alternate sources of ^{137}Cs cannot be fully ruled out, the presence of a large number of fission and activation products combined with the presence of, and the relative amounts of, ^{134}Cs suggested a fresh fission source.

The challenge with sparse environmental measurements and distant unacknowledged events is that several techniques are required to characterize the event and to delve into possible causes and the ultimate source of a release. Small radiological releases, the occurrence of which can be unknown to facility operators, may be observed at a distance with modern high-sensitivity radiation monitoring equipment. However, to fully characterize and understand these important events, they require multiple analysis techniques. This is particularly true for events involving radionuclides that are important to CTBT. In this event, detections of unusual radioisotopes were observed at multiple sites and countries. While the radioisotopes detected provided valuable information, it was not until more advanced techniques including autoradiography, high-resolution ATDM, reactor fuel burn-up models and coincidence spectroscopy that the necessary inferences could be made on the actual source of this event.

The initial observations of radioisotopes, comprised of both fission and activation products suggested the release came from a nuclear facility such as a NPP. The detection and non-detection of radionuclides of co-located samplers such as the one in Stockholm suggested that the particles released were discrete, small in number, and relatively large. Through coincident spectroscopy that showed anisotropy between the anthropogenic material and autoradiography the particle size distribution and overall darkening of the images confirmed this hypothesis. Furthermore, ATDM was useful to trace the general dynamics of the aerosol particles, but caution must be used with the interpretation of these models as particles with these characteristics are not easily modelled. The particle size distribution of the release was impossible to accurately characterize without additional information such as the actual mechanism of the release or near field collection sites. With a sparse detection network this information is not usually available. However, the use of ATDM allowed for the creation of a list of candidate facilities that could be evaluated in the assessment process.

The multi-detector configuration is a powerful tool to not only understand the composition of the debris on a filter, but also to understand the environmental (and ultimately the source) phenomenology

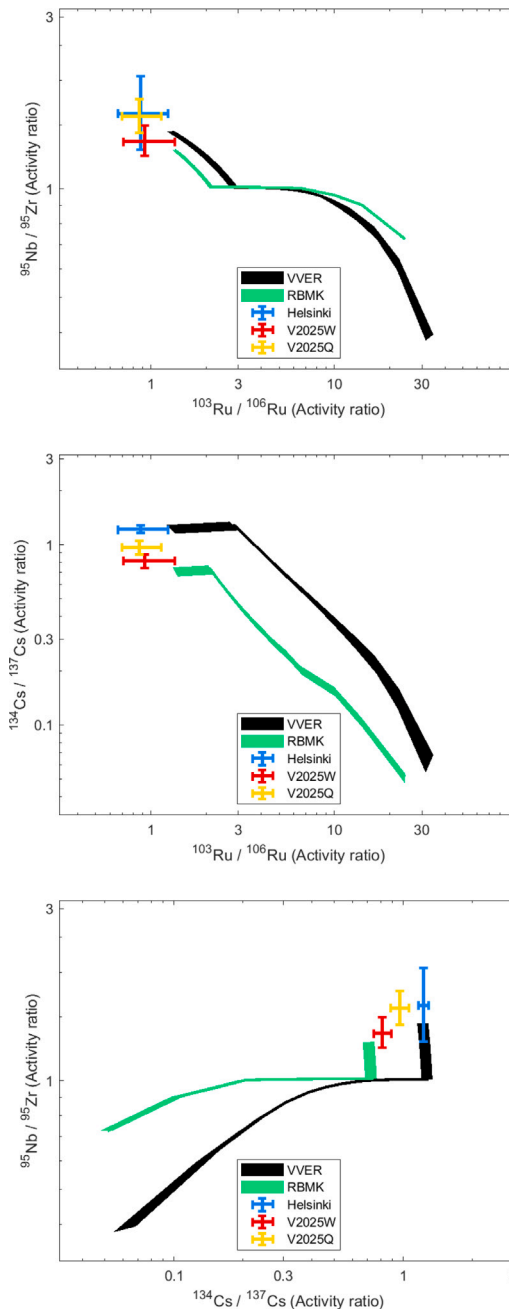


Fig. 9. The fuel burn-up from core insertion through to discharge and decay is shown for three different isotopes/isobars. The highest probability scenario in each case is shown. The Helsinki (whole and quarter sample) and Visby observed ratios are shown along with their associated uncertainty. The thickness of the fuel evolution shows the range of values possible due to the position of the fuel pin within the core.

that gave rise to the presence of the anthropogenic radionuclides. The radioactive particles were highly inhomogeneous in this case, and a simple analysis using a single detector could lead to misunderstanding the source or possibly the genesis time of the material as the isotopic clock could be inconsistent.

The combination of two detectors is robust against sample inhomogeneity. The dual detector measurement that measures both sample faces simultaneously gives a more robust estimate of the activity concentration. The anthropogenic radionuclides on the filter showed an inconsistent bias to one face (i.e. not all isotopes showed a favourable collection to one side of the filter). This would be due to both the airflow into the sampler and also the handling of the filter when

it is compressed into a puck for gamma ray spectroscopy measurement. Small differences in isotopic ratios may significantly change the interpretation of the data.

Considering the auto-radiographs in combination with the ratio analysis, the Helsinki sample was closest to being a pure VVER collection of aerosols. Visby showed evidence of either a RBMK or an admixture of VVER and RBMK sources. It is also possible that the presence of historical environmental ^{137}Cs was present in the sample which would have caused the sample to appear more like an RBMK collection. With both possibilities, it is difficult to speculate on a release of nuclear fuel material from two different reactor types so proximate

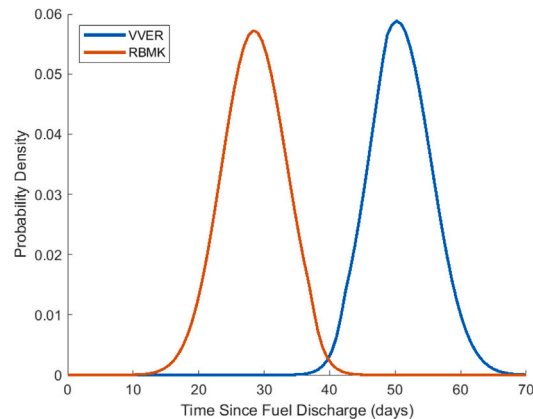


Fig. 10. Probability distribution of the time since fuel discharge for the two reactor types. From the ratio analysis, a VVER is the most likely source with the time since fuel discharge being 51 d.

in time versus the likelihood the Visby sample had ^{137}Cs present from another source.

The Helsinki sample based upon a ratio analysis of fission products, with a corresponding Maximum Likelihood Estimate (MLE) time since fuel discharge of approximately 51 d. The latter Visby sample (5) indicated a RBMK or a mixed RBMK-VVER source. The fuel burn-up analysis also indicates that there is very little overlap in discharge time between the two reactor types.

4. Conclusion

From the analysis presented here the most likely candidate for the source location of the unusual anthropogenic radionuclides observed in the Baltic region is from VVER, and possibly RBMK fuel located at the Leningrad nuclear plant. The VVER fuel would have been discharged from the reactor approximately 51 d prior to the release events. Normally, spent fuel from either reactor type would be immediately stored onsite in a pool for around five years before moving to dry storage. Without more information on actual plant conditions, it is difficult to say conclusively if activities at the Leningrad plant led to the release of these radionuclides and whether the release was related to the spent fuel pool.

The process to arrive at this conclusion was complicated as it involved the consideration of multiple types of analyses such as gamma ray spectroscopy with both single and multiple detectors, autoradiography, analysis of ATDM, an analysis of observed historical environmental activity concentrations of radionuclides, typically ^{137}Cs , and fuel burn-up models and the resulting analysis of activity ratio for several pairs.

This particular event has illustrated one cautionary factor that is involved when using ATDM with the transport of discrete particles during the event analysis process. When radioactivity is carried by a small number of particles, the normal models applied in ATDM are not appropriate as these models typically make an assumption of aerosols transport in a well-dispersed plume. In this study, this assumption was not valid, and was only determined through autoradiography and the use of a multi-detector system such as *Thin Man*. While the ATDM model will still have valuable information in identifying the possible origin, the use of these models in estimating source sizes would also overestimate the size of the release. The development of a transport model better able to deal with discrete particle would aid in the analysis of events, as sample inhomogeneity has been demonstrated previously during the Fukushima reactor accident (Gomez et al., 2014; Woods et al., 2013; Zhang et al., 2011). Improvements in uncertainty

estimation would also be beneficial for both particulate and noble gas releases (Hoffman et al., 2022).

The use of additional non-destructive analysis techniques for CTBT verification has been shown to have clear benefits in understanding the nature of events that involve anthropogenic radionuclide detections. These techniques are a source of invaluable information that can clarify the phenomenology and nature of an event. Furthermore, the techniques employed here are much more economical than conducting an OSI, in the event of inconclusive evidence. If a request for an OSI is granted it would involve a time-consuming and expensive process where inspectors designated by the CTBTO would inspect a 1000 km² designated location and begin a search for evidence of a nuclear test. Beyond being an expensive proposition, the conduct of an OSI is intrusive and much more complex. It is far more informative to exhaust all available sample measurement information. Should an OSI be necessary, the additional information gained from these techniques would better inform the OSI process.

Although a considerable amount of time has passed since the release and the request for information from IAEA member states, it is unlikely that confirmation of the source location and process that led up to the environmental release will be provided. Should new information, such as the date of refuelling or fuel rod failures, be available the assessment and conclusions from this analysis would be refined.

CRediT authorship contribution statement

Ian Hoffman: Writing – review & editing, Writing – original draft, Visualization, Software, Methodology, Investigation, Formal analysis, Data curation, Conceptualization. **P. Mekarski:** Writing – original draft, Methodology, Investigation, Formal analysis. **A. Botti:** Resources. **J. Yi:** Formal analysis. **A. Malo:** Resources. **C. Cochrane:** Visualization, Resources, Formal analysis. **V. Khotylev:** Formal analysis. **J. Kastlander:** Writing – original draft, Resources. **A. Axelsson:** Writing – original draft, Formal analysis. **A. Ringbom:** Resources. **M. Moring:** Resources. **T. Karhunen:** Resources. **A. Mattila:** Resources. **M. Goodwin:** Resources, Formal analysis. **A. Davies:** Resources, Formal analysis. **K. Ungar:** Writing – review & editing, Conceptualization.

Declaration of competing interest

The authors declare that they have no known competing financial interests or personal relationships that could have appeared to influence the work reported in this paper.

Data availability

Data will be made available on request.

References

- Altenmüller, K., Agostini, M., Appel, S., Bellini, G., Benziger, J., Berton, N., Bick, D., Bonfini, G., Bravo, D., Caccianiga, B., Calaprice, F., Caminata, A., Cavalcante, P., Chepurinov, A., Cribier, M., D'Angelo, D., Davini, S., Derbin, A., di Noto, L., Drachnev, I., Durero, M., Empl, A., Etenko, A., Farinon, S., Fischer, V., Fomenko, K., Franco, D., Gabriele, F., Gaffiot, J., Galbiati, C., Ghiano, C., Giammarchi, M., Göger-Neff, M., Goretta, A., Gromov, M., Hagner, C., Houdy, T., Hungerford, E., Ianni, A., Ianni, A., Jonqueres, N., Kaiser, M., Kobaychev, V., Korablev, D., Korga, G., Krynn, D., Lachenmaier, T., Lasserre, T., Laubenstein, M., Lehnert, B., Link, J., Litvinovich, E., Lombardi, P., Lombardi, P., Ludhova, L., Lukyanchenko, G., Machulin, I., Maneschg, W., Marocci, S., Maricic, J., Mention, G., Meroni, E., Meyer, M., Miramonti, L., Misiaszek, M., Montuschi, M., Muratova, V., Musenich, R., Neumair, B., Oberauer, L., Obolensky, M., Ortica, F., Pagani, L., Pallavicini, M., Papp, L., Perasso, L., Pocar, A., Ranucci, G., Razeto, A., Re, A., Roncin, R., Romani, A., Rossi, N., Schönert, S., Scola, L., Semenov, D., Simgen, H., Skorokhvatov, M., Smirnov, O., Sotnikov, A., Sukhotin, S., Suvorov, Y., Tartaglia, R., Testera, G., Toropova, M., Unzhakov, E., Veyssiére, C., Vivier, M., Vogelaar, R.B., von Feilitzsch, F., Wang, H., Winter, J., Wojcik, M., Wurm, M., Yokley, Z., Zaimidoroga, O., Zavatarelli, S., Zuber, K., Zuzel, G., 2016. The search for sterile neutrinos with SOX-borexino. *Phys. Atom. Nucl.* 79 (11), 1481–1484. <http://dx.doi.org/10.1134/S106377881610001X>.
- Britton, R., Davies, A., 2019. Limits of detection — Enhancing identification of anthropogenic radionuclides. *Nucl. Instrum. Methods Phys. Res. A* 947, 162818. <http://dx.doi.org/10.1016/j.nima.2019.162818>, URL: <https://www.sciencedirect.com/science/article/pii/S0168900219312598>.
- Charlton, W.S., Fearey, B.L., Nakhleh, C.W., Parish, T.A., Perry, R.T., Poths, J., Quagliano, J.R., Stanbro, W.D., Wilson, W.B., 2000. Operator declaration verification technique for spent fuel at reprocessing facilities. *Nucl. Instrum. Methods Phys. Res. B* 168 (1), 98–108. [http://dx.doi.org/10.1016/S0168-583X\(99\)00633-3](http://dx.doi.org/10.1016/S0168-583X(99)00633-3), URL: <https://www.sciencedirect.com/science/article/pii/S0168583X99006333>.
- Cooke, M.W., Botti, A., Zok, D., Steinhauser, G., Ungar, K.R., 2020. Identification of a chemical fingerprint linking the undeclared 2017 release of ^{106}Ru to advanced nuclear fuel reprocessing. *Proc. Natl. Acad. Sci.* 117 (26), 14703–14711. <http://dx.doi.org/10.1073/pnas.2001914117>.
- D'Amours, R., Malo, A., Flesch, T., Wilson, J., Gauthier, J.-P., Servranckx, R., 2015. The Canadian meteorological centre's atmospheric transport and dispersion modelling suite. *Atmosphere Ocean* <http://dx.doi.org/10.1080/07055900.2014.1000260>.
- Eslinger, P.W., Lowrey, J.D., Miley, H.S., Rosenthal, W.S., Schrom, B.T., 2019. Source term estimation using multiple xenon isotopes in atmospheric samples. *J. Environ. Radioact.* 204, 111–116. <http://dx.doi.org/10.1016/j.jenvrad.2019.04.004>, URL: <https://www.sciencedirect.com/science/article/pii/S0265931X19301778>.
- Fieller, E.C., 1954. Some problems in interval estimation. *J. R. Stat. Soc. Ser. B Stat. Methodol.* 16 (2), 175–185, URL: <http://www.jstor.org/stable/2984043>.
- Gomez, R., Biegalski, S., Woods, V., 2014. Aerosol sample inhomogeneity with debris from the fukushima daiichi accident. *J. Environ. Radioact.* 135, 1–5. <http://dx.doi.org/10.1016/j.jenvrad.2014.03.011>, URL: <http://www.sciencedirect.com/science/article/pii/S0265931X14000903>.
- Hoffman, I., Malo, A., Ungar, K., 2022. Uncertainty and source term reconstruction with environmental air samples. *J. Environ. Radioact.* 246, 106836. <http://dx.doi.org/10.1016/j.jenvrad.2022.106836>, URL: <https://www.sciencedirect.com/science/article/pii/S0265931X22000261>.
- Hopp, T., Zok, D., Kleine, T., Steinhauser, G., 2020. Non-natural ruthenium isotope ratios of the undeclared 2017 atmospheric release consistent with civilian nuclear activities. *Nature Commun.* 11 (1), 2744. <http://dx.doi.org/10.1038/s41467-020-16316-3>.
- IAEA, 2022. Nuclear data section. Retrieved from Isotope Browser Application.
- Istituto Nazionale di Fisica Nucleare, 2021. SOX - short distance oscillations with borexino. <https://home.infn.it/en/sox/13-esperimenti/2681-sox-short-distance-oscillations-with-borexino-ing>. Online (Accessed 16 September 2022).
- Krieger, H.L., Groche, D., 1960. Occurrence of scandium-46 and cesium-134 in radioactive fallout. *Science* 131 (3392), 40–42, URL: <http://www.jstor.org/stable/1704998>.
- Masson, O., Steinhauser, G., Zok, D., Saunier, O., Angelov, H., Babić, D., Bečková, V., Bieringer, J., Bruggeman, M., Burbidge, C.I., Conil, S., Dalheimer, A., De Geer, L.-E., de Vismes Ott, A., Eleftheriadis, K., Estier, S., Fischer, H., Garavaglia, M.G., Gasco Leonarte, C., Gorzkiewicz, K., Hainz, D., Hoffman, I., Hýža, M., Isajenko, K., Karhunen, T., Kastlander, J., Katzberger, C., Kierepko, R., Knetusch, G.-J., Kövendiné Kónyi, J., Lecomte, M., Mietelski, J.W., Min, P., Møller, B., Nielsen, S.P., Nikolic, J., Nikolovska, L., Penev, I., Petrincec, B., Povinec, P.P., Querfeld, R., Raimondi, O., Ransby, D., Ringer, W., Romanenco, O., Rusconi, R., Saey, P.R.J., Samsonov, V., Šilobritienė, B., Simion, E., Söderström, C., Šošarić, M., Steinkopff, T., Steinmann, P., Sýkora, I., Tabachnyi, L., Todorovic, D., Tomankiewicz, E., Tschiersch, J., Tsihranski, R., Tzortzis, M., Ungar, K., Vidic, A., Weller, A., Wershofen, H., Zagayvai, P., Zalewska, T., Zapata García, D., Zorko, B., 2019. Airborne concentrations and chemical considerations of radioactive ruthenium from an undeclared major nuclear release in 2017. *Proc. Natl. Acad. Sci.* 116 (34), 16750–16759. <http://dx.doi.org/10.1073/pnas.1907571116>.
- Osborn, J.M., Kitcher, E.D., Burns, J.D., Folden, III, C.M., Chirayath, S.S., 2018. Nuclear forensics methodology for reactor-type attribution of chemically separated plutonium. *Nucl. Technol.* 201 (1), 1–10. <http://dx.doi.org/10.1080/00295450.2017.1401442>.
- Parsons-Davis, T., Knight, K., Fitzgerald, M., Stone, G., Caldeira, L., Ramon, C., Kristo, M., 2018. Application of modern autoradiography to nuclear forensic analysis. *Forensic Sci. Int.* 286, 223–232. <http://dx.doi.org/10.1016/j.forsciint.2018.03.027>, URL: <https://www.sciencedirect.com/science/article/pii/S0379073818301245>.
- Ramebäck, H., Söderström, C., Granström, M., Jonsson, S., Kastlander, J., Nylén, T., Ågren, G., 2018. Measurements of ^{106}Ru in Sweden during the autumn 2017: Gamma-ray spectrometric measurements of air filters, precipitation and soil samples, and in situ gamma-ray spectrometry measurement. *Appl. Radiat. Isot.* 140, 179–184. <http://dx.doi.org/10.1016/j.apradiso.2018.07.008>, URL: <https://www.sciencedirect.com/science/article/pii/S0969804318301714>.
- Studs vik, A., 2008. HELIOS-2. <https://www.studsvik.com/what-we-do/products/helios-2/>. Online; (Accessed 12 September 2022).
- Vivier, M., Agostini, M., Altenmüller, K., Appel, S., Bellini, G., Benziger, J., Berton, N., Bick, D., Bonfini, G., Bravo, D., Caccianiga, B., Calaprice, F., Caminata, A., Cavalcante, P., Chepurinov, A., Choi, K., Cribier, M., D'Angelo, D., Davini, S., Derbin, A., Noto, L.D., Drachnev, I., Durero, M., Etenko, A., Farinon, S., Fischer, V., Fomenko, K., Franco, D., Gabriele, F., Gaffiot, J., Galbiati, C., Ghiano, C., Giammarchi, M., Goeger-Neff, M., Goretta, A., Gromov, M., Hagner, C., Houdy, T., Hungerford, E., Ianni, A., Ianni, A., Jonqueres, N., Jedrzejczak, K., Kaiser, M., Kobaychev, V., Korablev, D., Korga, G., Kornoukhov, V., Krynn, D., Lachenmaier, T., Lasserre, T., Laubenstein, M., Lehnert, B., Link, J., Litvinovich, E., Lombardi, F., Lombardi, P., Ludhova, L., Lukyanchenko, G., Machulin, I., Maneschg, W., Maneschg, W., Marocci, S., Maricic, J., Mention, G., Meroni, E., Meyer, M., Miramonti, L., Misiaszek, M., Montuschi, M., Mosteiro, P., Muratova, V., Musenich, R., Neumair, B., Oberauer, L., Obolensky, M., Ortica, F., Pallavicini, M., Papp, L., Perasso, L., Pocar, A., Ranucci, G., Razeto, A., Re, A., Romani, A., Roncin, R., Rossi, N., Schönert, S., Scola, L., Semenov, D., Skorokhvatov, M., Smirnov, O., Sotnikov, A., Sukhotin, S., Suvorov, Y., Tartaglia, R., Testera, G., Thurn, J., Toropova, M., Veyssiére, C., Unzhakov, E., Vogelaar, R.B., von Feilitzsch, F., Wang, H., Weinz, S., Winter, J., Wojcik, M., Wurm, M., Yokley, Z., Zaimidoroga, O., Zavatarelli, S., Zuber, K., Zuzel, G., collaboration, B., 2016. SOX: search for short baseline neutrino oscillations with borexino. *J. Phys. Conf. Ser.* 718 (6), 062066. <http://dx.doi.org/10.1088/1742-6596/718/6/062066>.
- Woods, V.T., Bowyer, T.W., Biegalski, S., Greenwood, L.R., Haas, D.A., Hayes, J.C., Lepel, E.A., Miley, H.S., Morris, S.J., 2013. Parallel radioisotope collection and analysis in response to the fukushima release. *J. Radioanal. Nucl. Chem.* 296 (2), 883–888. <http://dx.doi.org/10.1007/s10967-012-2210-3>.
- Zhang, W., Bean, M., Benotto, M., Cheung, J., Ungar, K., Ahier, B., 2011. Development of a new aerosol monitoring system and its application in fukushima nuclear accident related aerosol radioactivity measurement at the CTBT radionuclide station in sidney of Canada. *J. Environ. Radioact.* 102 (12), 1065–1069. <http://dx.doi.org/10.1016/j.jenvrad.2011.08.007>, URL: <http://www.sciencedirect.com/science/article/pii/S0265931X11001950>.
- Zhang, W., Ro, H., Liu, C., Hoffman, I., Ungar, K., 2017. Design and optimization of a dual-HPGe Gamma spectrometer and its cosmic veto system. *IEEE Trans. Nucl. Sci.* 64 (3), 894–900. <http://dx.doi.org/10.1109/TNS.2017.2654686>.